



Salicylic acid complexed with TiO₂ for visible light-driven selective oxidation of amines into imines with air

Xia Li^a, Hui Xu^a, Ji-Long Shi^a, Huimin Hao^a, Hong Yuan^b, Xianjun Lang^{a,*}

^a College of Chemistry and Molecular Sciences, Wuhan University, Wuhan 430072, China

^b Key Laboratory of Pesticide and Chemical Biology of Ministry of Education, College of Chemistry, Central China Normal University, Wuhan 430079, China

ARTICLE INFO

Keywords:

Surface complex
Photocatalysis
Titanium dioxide
Salicylic acid
Amines

ABSTRACT

The interplay of salicylic acid (SA) and reactive oxygen species (ROS) can modulate biotic and abiotic stress of plants, essential biological aerobic oxidation processes. Meanwhile, ROS plays a critical role in TiO₂ photocatalytic system for the degradation of organic species. Herein, we developed a system consisted of SA and TiO₂ aiming at the selective oxidation of organic molecules by ROS. Interestingly, SA complexed with TiO₂ leads to ligand-to-metal charge transfer (LMCT) under visible light irradiation. The charge transfer from ligand (chemically adsorbed SA) to metal (conduction band of TiO₂) activates O₂ to ROS, superoxide (O₂^{•−}). The positive charge located at ligand SA is connected with (2,2,6,6-tetramethylpiperidin-1-yl)oxyl (TEMPO) catalysis for direct two-electron oxidation of amines and later regenerated by O₂^{•−}. SA and its derivatives were screened as ligands of TiO₂ for the selective aerobic oxidation of amines into imines under blue light-emitting diode (LED) irradiation in which 5-CH₃O-SA (5-methoxysalicylic acid, 0.8 mol%) complexed with anatase TiO₂ and coupled with TEMPO (5 mol%) confers significantly better results than the others. By this visible light LMCT route, both primary amines and secondary amines can be selectively oxidized into corresponding imines with atmosphere O₂ as the terminal oxidant. Importantly, the desired product of *N*-benzylidenebenzylamine can be isolated in 92% yield.

1. Introduction

By volume, the atmosphere of Earth contains about 78% of N₂ and 21% of O₂ which means O₂ is in abundant supply that can be conveniently used as an oxidant in an economic and sustainable manner. Consequently, atmosphere O₂ is well established as the quintessential oxidant for oxidation of organic species [1,2]. However, spin barriers exist between the ground states of O₂ and other organic molecules which in turn maintain organic molecules stable and life possible on earth at the exposure of ubiquitous O₂ [3]. Life on Earth rests on the balance between the metabolism of O₂ and thermodynamically favored transformations of O₂ and organic molecules into CO₂ and H₂O. Lessons can be borrowed from evolution of biological systems to control the ROS during the metabolism of O₂. The interplay of SA and ROS can modulate biotic and abiotic stress of plants [4], the essential metabolism of O₂ processes. For example, SA was reported to induce both immediate spike and long lasting phases of oxidative burst in plant represented by the generation of ROS such as superoxide anion radical (O₂^{•−}) [5,6]. In preceding reports, O₂^{•−} was always regarded as the central ROS in connecting the photocatalytic and catalytic cycles and

therefore implemented the visible light-driven selective oxidation reactions [7–11]. Resultantly, we want to take advantage of the excellent regulation effects of SA on ROS to control the selectivity of photocatalytic oxidation reactions with atmosphere O₂.

TiO₂ is the emblematic photocatalyst with great potential in solving the urgent environmental and energy issues which has therefore been under intensive research effort for several decades. As we all know, TiO₂ has been favored for its outstanding properties such as stability, non-hazardousness, cheapness. Continuing effort is still centered on this excellent photocatalytic material. Even though visible light photocatalytic systems might be possible with TiO₂ as a reaction platform, this semiconductor photocatalyst cannot drive visible light reaction by itself due to lack of visible light absorption [12]. Thus, irradiation of UV light was usually needed to overcome the bandgap of TiO₂ for oxidative reactions [13]. Notable achievements have been realized in improving its visible light photocatalytic performance. For instance, many modification methods for TiO₂ nanomaterials have been used to enhance visible light absorption, including doping with transition metals [14], non-metals [15] and loading metal nanoparticles [16]. However, in many cases, visible light photocatalytic activities were achieved at the

* Corresponding author.

E-mail address: xianjunlang@whu.edu.cn (X. Lang).

<https://doi.org/10.1016/j.apcatb.2018.11.090>

Received 6 September 2018; Received in revised form 15 November 2018; Accepted 29 November 2018

Available online 29 November 2018

0926-3373/© 2018 Elsevier B.V. All rights reserved.

expense of UV-driven activity in scenario like the doping of TiO₂ bulk materials. Under this circumstance, surface modification of TiO₂ with small organic molecules is an emerging approach and has been used to improve their performance in utilizing the energy of solar light [17–19]. Both TiO₂ and small organic molecules do not absorb visible light separately. However, after their interaction, surface complex would be formed, giving rise to visible light-driven LMCT and subsequent oxidation reactions.

To assemble a visible light photocatalytic reaction system via LMCT, organic molecules such as catechol and its derivatives have been explored as prevailing surface ligands to modify TiO₂. They can be firmly fixed onto the surface of TiO₂ by the mode of chemical adsorption which in turn can guarantee a favorable efficiency for electron transfer [20]. Hence, these surface complexes had been adopted in many aspects of photocatalytic applications. For example, visible light photocatalytic H₂ production on catechol-TiO₂ hybrids [21], degradation of organic contaminants [22] and reduction of inorganic heavy metal ions [23] on hydroxynaphthalene-modified TiO₂ were unearthed. Very recently, our research group discovered a visible light-driven protocol for selective aerobic oxidation of amines into imines on catechol-TiO₂ complex photocatalyst [24], which in turn offers a new perspective for us to understand and apply this interfacial electron transfer process for the purpose of organic transformations.

Stimulated by this prior success, we want to find new ligands and apply them via the mode of LMCT for the photocatalytic selective oxidation of amines with atmosphere O₂. In the pursuit of innovative ligand, many theoretical and experimental investigations were conducted mainly on surface modification of TiO₂ with catechol and its derivatives. Only a few papers focus on the binding of SA on the surface of TiO₂. Like catechol and its derivatives, SA also has a small molecular structure, which supplies an equally favorable model for further investigation on the charge-transfer (CT) complexes; second, SA can be incorporated with TiO₂ by chemical absorption through an ester-like bond conjunction which makes sure smooth interfacial electron transfer from SA to the conduction band of TiO₂; third, TiO₂ modified by SA can increase its dispersion in organic solvent by reducing the hydrophilicity of TiO₂ [25–28]. Furthermore, due to the small molecular structure of SA, it supplies a favorable model for in depth investigation on the details of the interaction between an organic molecule and TiO₂ surface. These interplays between SA, TiO₂ and ROS make SA a good choice as a surface ligand. However, the degradation of SA on TiO₂ based materials had already been presented in some preceding reports [29,30], suggesting that SA and its derivatives are very fragile under the assault of ROS during the course of photocatalytic aerobic oxidation. Like the case with catechol or its derivatives as the ligand, preserving the stability of SA on TiO₂ surface at a reasonable duration of time under visible light irradiation should be considered beforehand. There was little information about selective aerobic oxidation based on surface complex. One reason is that selectivities in the photocatalysis-promoted transformations of organic molecules are difficult to control [31]. In addition, surface complex can be easily destroyed in photocatalytic systems. Another reason is that the details of charge transfer and binding dynamics on the surface of TiO₂ is still unclear. Taking these factors into consideration, surface complex photocatalysis for selective oxidation of organic molecules is a formidable challenge. To address these challenges, we adopted a strategy of cooperative photocatalysis to accelerate the charge transfer process [32,33].

In this paper, we report a highly efficient visible light photocatalytic system for the selective oxidation of amines into imines with air by merging SA-TiO₂ complex photocatalysis with TEMPO catalysis. For the reaction, we chose SA to form a surface complex with TiO₂. In view of our previous experience, TEMPO was adopted a co-catalyst to maintain the stability of the photocatalytic system which removes the charge stress upon SA-TiO₂ complex photocatalyst. More interestingly, our finding shows that 5-CH₃O-SA can markedly increase the photocatalytic activity by inducing a significant red-shift in the optical

absorption region due to CT sensitization. Compared with the previous work we done with catechol-TiO₂ complex, 5-CH₃O-SA-TiO₂ enables a much better result. Apart from primary amines, many kinds of secondary amines can also be selectively oxidized, alluding the importance of more innovative selection of ligands in the LMCT for visible light-driven organic transformations.

2. Experimental section

2.1. Reagents and solvents

Reagents were supplied by the companies such as Sigma-Aldrich, Alfa Aesar and TCI, J&K Scientific, etc. The solvents were supplied by Merck, Fischer Scientific and Sinopharm Chemical Reagent Co. Ltd., China. Ishihara ST-01 TiO₂ was supplied from Ishihara Sangyo Kaisha, Ltd., Japan. Benzyl- α,α -d₂-amine was procured from CDN Isotopes, Quebec, Canada. All the reagents and solvents were obtained from commercial suppliers and used without further purification.

2.2. Procedure for the photocatalytic selective oxidation of amine with air

The SA-TiO₂ complex was prepared *ex situ* and *in situ* according to previous report with some modifications [34]. The XRD and TEM, HRTEM characterizations are presented in Figure S3 and Figure S4. The operation for the photocatalytic selective oxidation of amine with air follows these steps. Firstly, place 50 mg of anatase TiO₂, 0.0024 mmol of 5-CH₃O-SA, 0.0015 mmol of TEMPO, 0.3 mmol of benzylamine and 1 mL of CH₃CN in a 10 mL Pyrex reactor with a butyl rubber septum for 5 min of ultrasonication. Secondly, stir the mixture in dark for 1 h to reach adsorption-desorption equilibrium. Thirdly, put the Pyrex reactor under a magnetic stirring apparatus. Mixture in the Pyrex reactor was stirred at 1500 rpm and irradiated with 3 W blue light-emitting diodes (LEDs). In this step, it is worth noting that the butyl rubber septum was punched with a hole by a rubber hole puncher to connect the reaction mixture with air. The temperature of the reaction system was controlled at 25 °C. Finally, the photocatalyst nanoparticles were separated from the reaction mixture by centrifugation. And the reaction product was analyzed by gas chromatography equipped with a flame ionization detector (GC-FID) using chlorobenzene as the internal standard. The structures of products were confirmed by comparison with the retention time with authentic samples by GC-FID and further confirmed by gas chromatography-mass spectrometry (GC-MS).

3. Results and discussion

Unlike catechol and its derivatives, the interfacial interaction between SA and TiO₂ was not abundantly investigated, and the application of this interaction was much less exploited as well. Besides, their interfacial properties were quite different. Femtosecond transient absorption established that CT excitation of catechol-TiO₂ was localized whilst the nature of CT excitation for SA-TiO₂ was delocalized [35]. It would be very interesting to investigate the surface complex photocatalysis of SA-TiO₂ for visible light-driven selective aerobic oxidation of amines, aiming at deepening the understanding of these processes and discovering better result than our previous one [24]. With this information in mind, we commenced to carry out a series of control experiments to establish the protocol for visible light-driven oxidation of benzylamine with air via LMCT with SA as the ligand for TiO₂ surface. The detailed results are presented in Fig. 1. Benzylamine itself does not undergo photochemical reaction (Fig. 1a). However, benzylamine can be complexed to TiO₂ that causes its self-oxidative coupling to imine with air [36]. But the conversion of benzylamine is very low under the control conditions (Fig. 1b). SA and TEMPO or their combination does not induce the oxidation of benzylamine under blue LED irradiation (Fig. 1c–e). Adding TEMPO to the benzylamine-TiO₂ complex system gives a very minimum promoting effect (Fig. 1f). With SA-

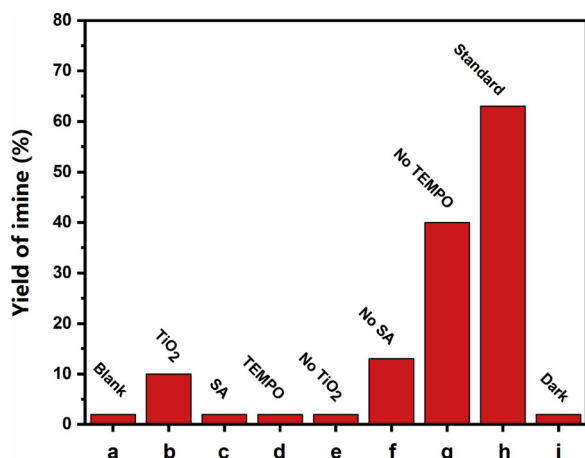


Fig. 1. Control experiments for the selective oxidation of amines into imines. (a) blank reaction; (b) TiO₂ only; (c) SA only; (d) TEMPO only; (e) without TiO₂; (f) without SA; (g) without TEMPO; (h) standard conditions; (i) dark condition.

Standard conditions: benzylamine (0.3 mmol), SA (2.4×10^{-3} mmol), TiO₂ (50 mg), TEMPO (0.0015 mmol), air (1 atm), CH₃CN (1 mL), blue LED irradiation (3 W \times 4), 1 h, yield of imine (*N*-benzylidenebenzylamine) was determined by GC-FID using the chlorobenzene as the internal standard.

TiO₂ complex as a photocatalyst, apparently improved yield of imine was observed (Fig. 1g). Moreover, about 50% increase of imine yield was achieved with 5 mol% of TEMPO as a co-catalyst (Fig. 1h). But the reaction can be completely switched off without blue LED irradiation (Fig. 1i), indicating the photocatalytic nature of the reaction.

Preliminary results in Fig. 1 demonstrate that one can conduct the visible light-driven oxidation of benzylamine into imine with air by merging the SA-TiO₂ complex photocatalysis and TEMPO catalysis. To further improve the system, we investigated the influence of different hydroxybenzoic acid ligands onto TiO₂ surface to form complex photocatalysts. Table 1 indicates that the *o*-, *m*- and *p*-positions of the two anchoring hydroxyl and carboxylic acid groups do not play a significant role in altering the photocatalytic selective oxidation of benzylamine into imine with air in the presence of 5 mol% of TEMPO as a co-catalyst. From a different point of view, this is quite a remarkable result to demonstrate that the scope of ligands for TiO₂ surface can be quite large, leaving much room for further development of surface complex photocatalysis with the strategy of visible light-driven LMCT.

It is quite exciting to find new ligands with TiO₂ for the creation of surface complex photocatalyst. But we were not satisfied with the visible light photocatalytic activity at hand. Stimulated by our recent work catechol surface complexed TiO₂, we knew that even the simple molecular structure surface complexes also can gain an excellent result for the visible light-driven oxidation of benzylamine with air. So we adopted SA to further study the interfacial charge transfer and binding

dynamics occurrence on the surface of TiO₂. To this end, we continued the pursuit of new ligands based on SA and its substituted derivatives (Fig. 2).

In view of our previous understanding, we studied the influence of substituted groups of SA on the photocatalytic selective oxidation of benzylamine with air (Table 2). There are two positions in the phenyl ring of SA that can be occupied by substituted group, i.e. the position 4 and the position 5. We used an electron-withdrawing group of -Br also to be in the position 4 and the position 5, 4-Br-SA and 5-Br-SA and an electron-donating group of -OCH₃ to be in the position 4 and the position 5 of SA, 4-CH₃O-SA and 5-CH₃O-SA. The conversions of benzylamine with these three ligands namely 4-Br-SA, 5-Br-SA and 4-CH₃O-SA just have slight variations compared with SA (entry 1 vs. entries 2–4, Table 2). We were surprised to find that the electron-donating group of -OCH₃ anchored in the position 5 of SA, 5-CH₃O-SA gave the best results, delivering the conversion of benzylamine up to 77% in 35 min (entry 5, Table 2). This is very different from our previous work of catechol surface complexed TiO₂ visible light photocatalysis for selective oxidation of amines, in which, electron-withdrawing groups promoted the conversion of benzylamine [24]. Conversely, in this work, electron-donating group in SA can tremendously enhance the conversion of benzylamine with air as the terminal oxidant. Moreover, in the two anchoring groups of SA, the phenyl hydroxyl group is the more important one. Even though ligand 5-CH₃O-SA is very similar to 4-CH₃O-SA, the substituted CH₃O-group relative to the phenyl hydroxyl group is very dissimilar. The former one is in a *para* position while the later one is in a *meta* position. The *para* substituted CH₃O-group has an electron-donating effect, while the *meta* substituted one does not have an apparent electronic effect. The electronic difference might engender the apparently better activity of 5-CH₃O-SA-TiO₂ than that of 4-CH₃O-SA-TiO₂.

The formation of the inner-sphere CT complex results in a broader red-shift of the absorption for 5-CH₃O-SA-TiO₂ compared to SA-TiO₂. This matches well with the DR-UV-vis spectra (Fig. 4a). According to Fig. 4a, the bandgaps of SA-TiO₂ and 5-CH₃O-SA-TiO₂ complexes are 2.5 eV and 2.3 eV respectively. For type II sensitization, the sensitizer does not undergo an excited state. Thus the conduction band potential of these two complexes is the same as that of anatase TiO₂, -0.5 V (vs. NHE). Therefore, the ground states of SA-TiO₂ and 5-CH₃O-SA-TiO₂ complexes are 2.0 V and 1.8 V (vs. NHE) respectively which are well above the valence band of TiO₂ (2.7 V vs. NHE). The better visible light absorption of 5-CH₃O-SA-TiO₂ than SA-TiO₂ makes it a better photocatalyst under longer wavelength light irradiation (entry 1 vs. entry 2, Table S1). However, without TEMPO, the outcome of reaction differs little when we performed control experiments with SA-TiO₂ and 5-CH₃O-SA-TiO₂ (entry 3 vs. entry 4, Table S1), suggesting that visible light absorption did not lead to different activities. Consequently, we attributed this particularly good result to the better cooperation between the photocatalytic and the catalytic cycles.

However, the different tendency of electronic effect of the substitutes between SA and catechol ligands is still unclear, which gives us

Table 1

The influence of different hydroxybenzoic acid ligands on the visible light photocatalytic selective oxidation of benzylamine with air ^[a].

<div style="text-align: center;"> </div>			
Entry	Ligand	Conv. [%] ^[b]	Sel. [%] ^[b]
1	SA (<i>o</i> -Hydroxybenzoic acid)	63	99
2	<i>m</i> -Hydroxybenzoic acid	62	93
3	<i>p</i> -Hydroxybenzoic acid	69	97

[a] Reaction conditions: benzylamine (0.3 mmol), hydroxybenzoic acid (2.4×10^{-3} mmol), TiO₂ (50 mg), TEMPO (0.015 mmol), air (1 atm), blue LED irradiation (3 W \times 4), CH₃CN (1 mL), 1 h. [b] Determined by GC-FID using chlorobenzene as the internal standard, conversion of benzylamine, selectivity of *N*-benzylidenebenzylamine.

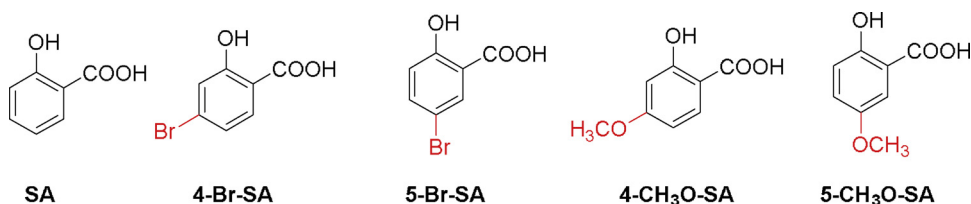


Fig. 2. The chemical structures of SA and its derivatives.

Table 2

The influence of SA and its derivatives on the visible light photocatalytic selective oxidation of benzylamine with air^[a].

Entry	Ligand	Conv. [%] ^[b]	Sel. [%] ^[b]
1	SA	29	99
2	4-Br-SA	23	99
3	5-Br-SA	29	99
4	4-CH ₃ O-SA	26	99
5	5-CH ₃ O-SA	77	98

[a] Reaction conditions: benzylamine (0.3 mmol), SA and its derivatives (0.0024 mmol), TiO₂ (50 mg), TEMPO (0.015 mmol), air (1 atm), blue LED irradiation (3 W × 4), CH₃CN (1 mL), 35 min. [b] Determined by GC-FID using chlorobenzene as the internal standard, conversion of benzylamine, selectivity of N-benzylidenebenzylamine.

Table 3

Comparison between the SA and catechol ligands on the visible light photocatalytic selective oxidation of benzylamine with air^[a].

Entry	Ligand	Conv. [%] ^[b]	Sel. [%] ^[b]
1	SA	41	99
2	CAT	44	90
3	5-CH ₃ O-SA	85	98
4	4-CN-CAT	53	98

[a] Reaction conditions: benzylamine (0.3 mmol), ligand (2.4×10^{-3} mmol), TiO₂ (50 mg), TEMPO (0.015 mmol), air (1 atm), blue LED irradiation (3 W × 4), CH₃CN (1 mL), 40 min. [b] Determined by GC-FID using chlorobenzene as the internal standard, conversion of benzylamine, selectivity of N-benzylidenebenzylamine.

a lot of room to improve it in future investigations. To unambiguously validate that the best SA derivative is a much better ligand than catechol and derivative for TiO₂ surface in terms of photocatalytic activity, we carried out further control experiments. Table 3 shows that CAT (catechol) was slightly better than SA. However, 5-CH₃O-SA contributed a significantly better than 4-CN-CAT (3,4-dihydroxybenzonitrile), the best catechol derivative for the oxidation of benzylamine with air [24], indicative of the importance of ligand selection in the formation of surface complex and the photocatalytic activity via LMCT under visible light irradiation.

Having established the best system with 5-CH₃O-SA-TiO₂ photocatalyst, we conducted a series of condition optimization experiments. Firstly, we chose several inert organic solvents and found that the effect of solvents on experiment is not obvious (Table S2). Therefore, we chose CH₃CN as solvent for the best result. The amounts of CH₃CN were also investigated (Table S3), suggesting that a concentrated benzylamine does not inhibit the reaction, even slightly favored. This is also very remarkable considering the photochemical reactions usually favor dilute conditions. Due to TiO₂ is a requisite ingredient of the CT complex, we explored the influence of the amount TiO₂ (Table S4). We further demonstrated that the adsorption mode of the SA and 5-CH₃O-SA onto TiO₂ attenuated total reflection Fourier transform IR (ATR-FTIR) spectroscopy (Fig. 3). The adsorption of SA onto TiO₂ nanoparticles leads to disappearance of the free SA bands at 1654, 1324, 1292, 1208, and 1187 cm⁻¹ and the shift of the band at 1246 cm⁻¹ to the lower frequency band at 1235 cm⁻¹. Since these bands correspond

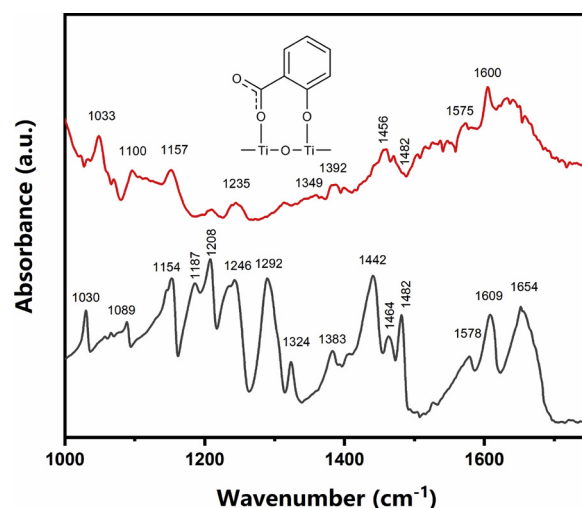


Fig. 3. ATR-FTIR spectra of SA-TiO₂ and free SA.

to vibrations of phenolic OH and carboxylic COOH groups, it is obvious that SA was complexed with TiO₂ by interaction of carboxyl and hydroxy oxygen with Ti atoms on the surface of TiO₂ [37]. Importantly, the adsorption mode of SA onto TiO₂ and the formation of complex was supported by density functional theory (DFT) calculations as well [38].

The Brunauer–Emmett–Teller (BET) specific surface areas for TiO₂, SA-TiO₂ and 5-CH₃O-SA-TiO₂ are 275, 265 and 262 m² g⁻¹ respectively. The XRD characterizations of these three complex photocatalysts are in Figure S3. Both the surface areas and the intrinsic diffraction properties of these complexes vary little and therefore could not lead to photocatalytic activity differences amongst different samples. UV–vis spectroscopy indicates the enhancement of TiO₂ optical properties owing to modification of its surface with SA and 5-CH₃O-SA through extending the range of visible light absorption through formation of titanium (IV) CT complexes. What's more, the absorbance area of 5-CH₃O-SA-TiO₂ overlaps with the light emitting spectrum of blue LED (Figure S5), further improving the overall efficiency of the photocatalytic system for organic transformation (Fig. 4b). We established that 5-CH₃O-SA-TiO₂ complex presents an excellent photocatalytic activity for selective oxidation of amines with air. Under standard

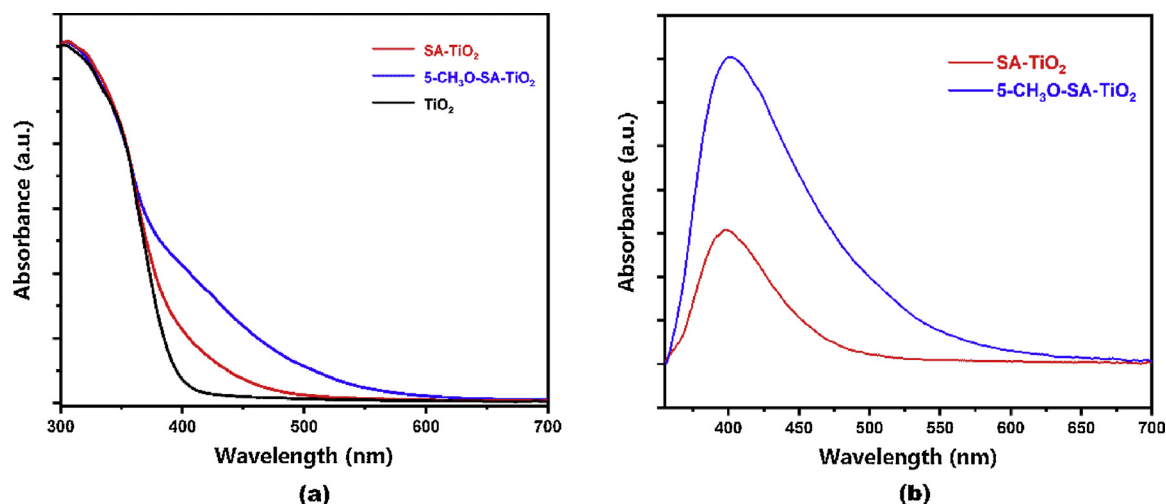


Fig. 4. Diffuse reflectance UV-vis spectra of (a) SA-TiO₂, 5-CH₃O-SA-TiO₂, TiO₂; (b) the UV-vis light absorbance of SA-TiO₂ and 5-CH₃O-SA-TiO₂ surface complexes.

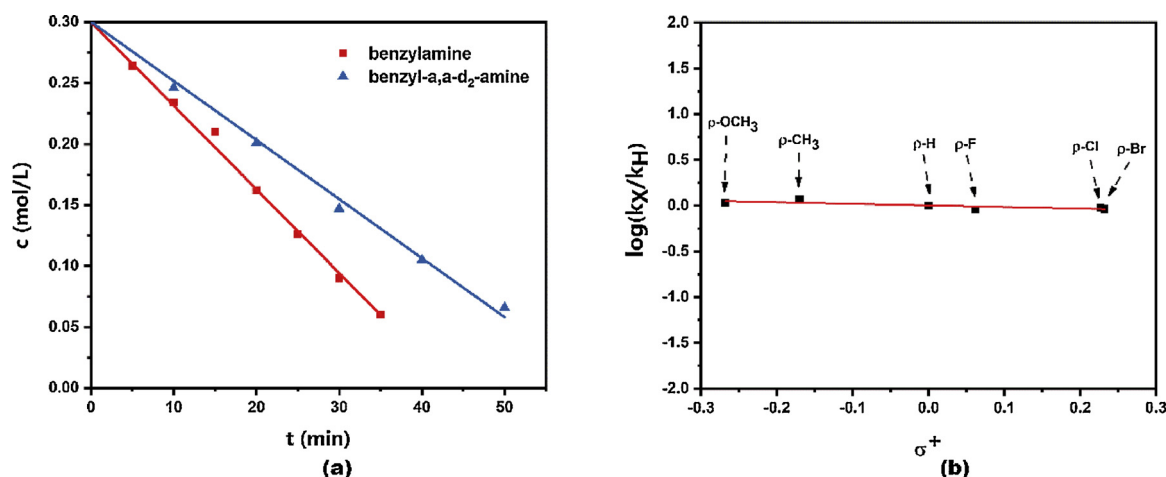


Fig. 5. Reaction kinetic studies on visible light-driven selective oxidation of amines with air by merging the 5-CH₃O-SA-TiO₂ complex photocatalysis with TEMPO catalysis (a) the selective oxidation of benzylamine (squares), the selective oxidation of benzyl-α,α-d₂-amine (triangles); (b) Hammett plot for the oxidation of *para*-substituted benzyl amines. Reaction conditions: benzylamines (0.3 mmol), 5-CH₃O-SA (0.0024 mmol), TEMPO (0.0015 mmol), air (1 atm), blue LED irradiation (3 W × 4), CH₃CN (1 mL).

Table 4

Quenching experiments to determine the ROS for the visible light photocatalytic oxidation of benzylamine ^[a].

Entry	Quencher (equiv.)	Roles	Yield [%] ^[b]
1	N ₂ (–)	O ₂ replacement	9
2 ^[c]	<i>p</i> -BQ (0.2)	O ₂ ^{•–} scavenger	4
3	AgNO ₃ (1)	electron scavenger	13
4 ^[d]	CD ₃ CN (–)	singlet oxygen maintainer	64

[a] Reaction conditions: benzylamine (0.3 mmol), 5-CH₃O-SA (2.4 × 10^{−3} mmol), TiO₂ (50 mg), TEMPO (0.015 mmol), CH₃CN (1 mL), blue LED irradiation (3 W × 4), 35 min. [b] Determined by GC-FID using chlorobenzene as the internal standard, yield of *N*-benzylidenebenzylamine. [c] *p*-BQ, *p*-benzoquinone. [d] CD₃CN (1 mL).

conditions, the conversion of benzylamine was as high as 77% after 35 min of reaction time on 5-CH₃O-SA-TiO₂ complex photocatalyst and TEMPO co-catalyst. And we found that each component of the cooperative photocatalytic system is essential. Without any part of them, the photocatalytic system would be inefficient, or stop working. Due to 5-CH₃O-SA-TiO₂ complex gives the best result for the selective aerobic oxidation under blue LED irradiation. We would use it throughout the subsequent experiments.

Thus, we carried out extra control experiments for selective oxidation of benzylamine with air by merging 5-CH₃O-SA-TiO₂ complex photocatalysis with TEMPO catalysis (Figure S1). The results more clearly indicate a genuine cooperative photocatalysis system is at work for this oxidation reaction. Furthermore, to ambiguously prove the central role of TEMPO in this system, we carried out experiments on the influence of the amounts of TEMPO on the selective photocatalytic aerobic oxidation of benzylamine (Table S5). The results make evident that catalytic amounts of TEMPO can increase the selectivity for imine and increase conversion for benzylamine nearly three-fold. Next, we surveyed the impact of different LEDs on the photocatalytic oxidation of benzylamine with air (Table S6). Excluding the difference in power output, better overlap of light emitting spectrum of the LED with the photocatalyst can give better results. The violent LED gives the best result. But small amount of UV light is present in its light-emitting spectrum which is an unattractive feature. Blue LED is the best choice of light source for the investigation of TiO₂ complex photocatalysis.

Next, we carried out a suite of kinetic studies for an insight of the reaction mechanism. The kinetic studies indicated that the visible light-driven selective oxidation benzylamine conforms to the characteristics of zero order reaction kinetics with a reaction rate constant *k_H* of 0.00696 mol·L^{−1}·min^{−1} (Fig. 5, a, blue line). The oxidation of benzyl-α,α-d₂-amine follows the same reaction order with a reaction rate

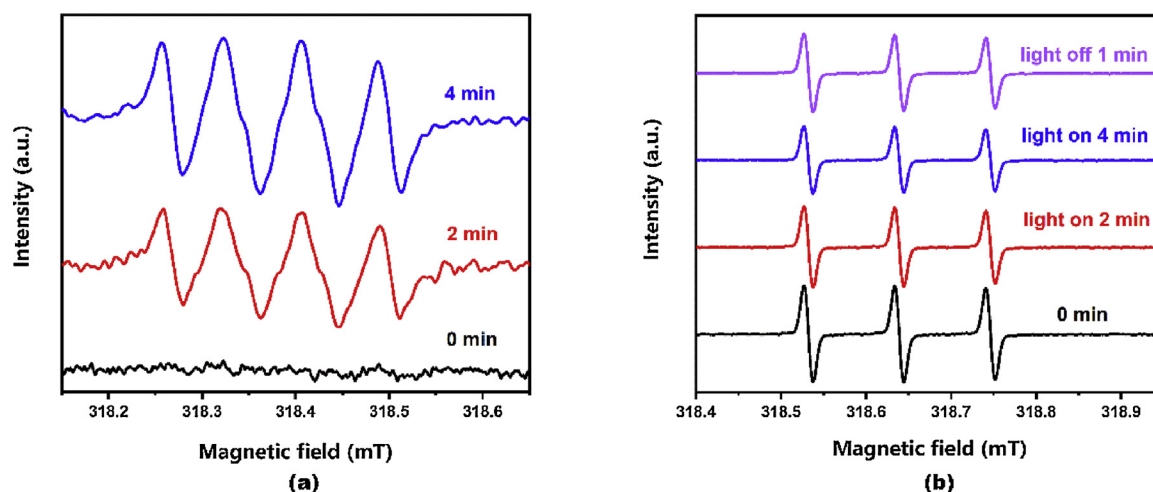


Fig. 6. The ESR spectra recorded during the visible light-driven selective oxidation of benzylamine by 5-CH₃O-SA-TiO₂ complex photocatalysis (a) spin trapping of superoxide radicals (O₂^{•-}) with DMPO (5,5-dimethyl-1-pyrroline *N*-oxide), (b) TEMPO.

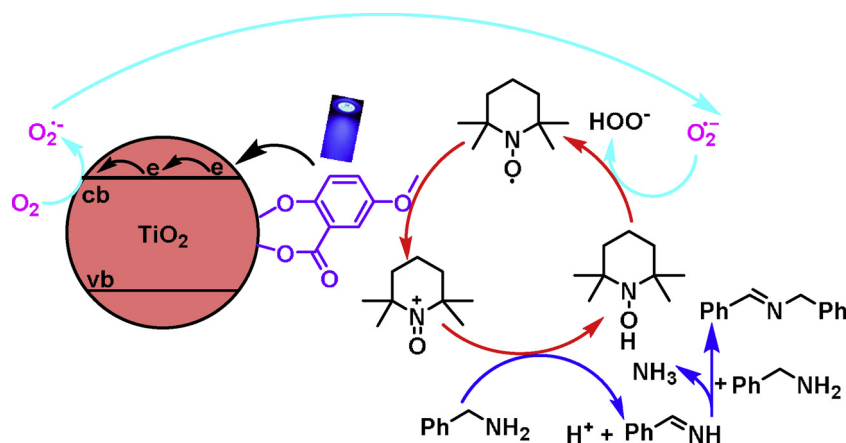


Fig. 7. The plausible mechanism for the visible light-driven selective oxidation of benzylamine with air by merging 5-CH₃O-SA-TiO₂ complex photocatalysis with TEMPO catalysis.

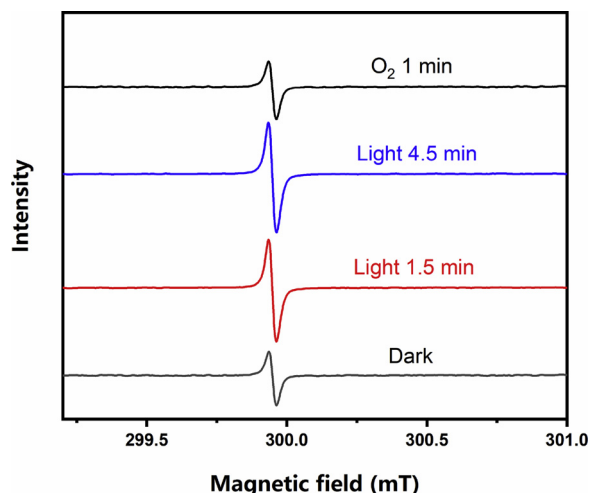


Fig. 8. The ESR spectra of conduction band electrons of 5-CH₃O-SA-TiO₂ complex under visible light irradiation (77 K).

constant k_D of $0.00471 \text{ mol} \cdot \text{L}^{-1} \text{ min}^{-1}$ (Fig. 5, a, red line). Therefore, we can calculate that the kinetic isotope effect (KIE) value k_H/k_D is 1.48, showing that the abstraction of C_α-H by 2,2,6,6-tetramethylpiperidine-1-oxoammonium (TEMPO⁺) has some impact but

does not impart a decisive effect on the whole reaction for the photocatalytic selective oxidation of benzylamine. This result can be interpreted that hydride was not involved in the abstraction of C_α-H step. In line with this result, the obtained Hammett plot (kinetic curves, Fig. S2) suggests that a not very cationic radical participates in the reaction process after the abstraction of C_α-H step (Fig. 5, b).

Quenching experiments could confirm the nature of ROS during the photocatalytic reaction (Table 4). The reaction does not proceed in an atmosphere of N₂, indicating that O₂ is the terminal oxidant for this reaction (entry 1, Table 4). *p*-BQ is a special reagent for trapping O₂^{•-}. And we can clearly see that the reaction does not occur in the presence of 0.2 equiv. of *p*-BQ (entry 2, Table 4), suggesting that this reaction is sustained by ROS, O₂^{•-}. AgNO₃ is an electron accepting competitor to O₂. When 1 equiv. of AgNO₃ was added to the system, both the conversion for benzylamine and the selectivity for imine were significantly dropped (entry 3, Table 4), which is owing to perturbation of the formation of O₂^{•-}. Conduction band electrons were partially intercepted by Ag⁺ rather than O₂. Moreover, when we replaced CH₃CN with CD₃CN, which is a singlet oxygen maintainer, as the solvent of this reaction, the conversion of benzylamine just slightly dropped (entry 4, Table 4), confirming that singlet oxygen does not get involved in the formation of imine. In addition, we investigated the influence of the initial O₂ pressures on the selective oxidation of benzylamine (Table S7). It was found that high O₂ pressure could assist the visible light photocatalytic selective oxidation processes, but this effect disappears

Table 5Visible light-driven selective oxidation of primary amines into imines with air by merging **5-CH₃O-SA-TiO₂** complex photocatalysis with TEMPO catalysis^[a].

$2 \text{ R-CH}_2\text{NH}_2 \xrightarrow[\text{CH}_3\text{CN, blue LEDs, air (1 atm)}]{\text{5-CH}_3\text{O-SA-TiO}_2, \text{TEMPO}} \text{R-CH=N-CH}_2\text{R}$					
Entry	Substrate	Product	T(h)	Conv. [%]	Sel. [%]
1			1.0	96	98
2 ^[c]			3.5	98	98
3			1.0	98	98
4			1.0	98	98
5			1.0	92	99
6			0.8	99	99
7			0.8	97	99
8			1.2	90	92
9			1.0	97	97
10			1.0	96	97
11			1.0	97	98
12			1.2	96	95
13			1.5	96	94

[a] Reaction conditions: primary amine (0.3 mmol), **5-CH₃O-SA** (0.0024 mmol), TiO₂ (50 mg), TEMPO (0.0015 mmol), air (1 atm), blue LED irradiation (3 W × 4), CH₃CN (1 mL). [b] Determined by GC-FID using chlorobenzene as the internal standard, conversion of primary amine, selectivity of corresponding imine. [c] Benzylamine (0.9 mmol), TEMPO (0.045 mmol).

at a certain pressure.

Superoxide anion O₂^{•−} is a very common ROS in biological and chemical systems. But O₂^{•−} is not a potent ROS in attacking neutral organic species but can efficiently oxidize hydroxylamine [39]. While hydroxylamine is the one species, 2,2,6,6-tetramethylpiperidin-1-ol (TEMPOH), during the catalytic cycle of TEMPO, providing perfect opportunity to connect with ROS of O₂^{•−}. In principle, TEMPOH can be the same as TEMPO as the starting co-catalyst. Indeed, when we used the same amount of TEMPOH as the co-catalyst, almost the same results was acquired. When we used TEMPO⁺BF₄[−] to substitute TEMPO, better result for the selective oxidation of benzylamine was obtained. In this visible light photocatalytic reaction, O₂^{•−} is the main ROS instead of singlet oxygen, which is firmly verified by electron spin resonance (ESR) spectra (Fig. 6a). The characteristic signal produced by 5,5-dimethyl-1-pyrroline *N*-oxide (DMPO) trapped O₂^{•−} increased as time went on. This means O₂^{•−} was produced continuously during the reaction process of visible light-driven aerobic oxidation of benzylamine. Fig. 6b shows the signal peak of TEMPO variations during the photocatalytic course. The signal was getting weaker with the reaction carrying on. This is because TEMPO (an ESR active species) is converted partially into ESR inactive species like TEMPO⁺ and TEMPOH, which is consistent with the mechanism we put forward. All of these experiments (Table 4), together with subsequent ESR experiments, have testified that O₂^{•−} is the essential ROS during the current photocatalytic selective oxidation of benzylamine.

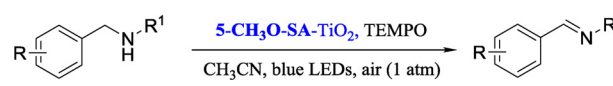
Investigations of semiconductor photocatalytic systems other than TiO₂ could have implications to understand our system [40–45]. With the increasing attention to the application of surface complex in photocatalysis, more details of the behavior such as binding mode, charge transfer manner, and electronic structure etc., between the modifier and the surface of TiO₂ were uncovered. On the basis all of the obtained results and in view of others' reports, a plausible reaction mechanism

for the visible light-driven selective oxidation of amine with air by merging **5-CH₃O-SA-TiO₂** complex photocatalysis with TEMPO catalysis has been arrived (Fig. 7). Unlike type I dye sensitization, in the case of **5-CH₃O-SA** sensitization, a new visible light absorption band is formed and the electron is directly photo-excited into the conduction band of TiO₂ without experiencing a CT excited state. This means electron can be transferred from the highest occupied molecular orbital (HOMO) of adsorbate to conduction band of TiO₂, leaving radical cation at the **5-CH₃O-SA** surface complex. Then TEMPO interacts with radical cation generated on the surface of **5-CH₃O-SA-TiO₂** complex photocatalyst to prevent it from being destroyed by ROS. Then TEMPO turns into TEMPO⁺. It is that TEMPO⁺ oxidizes benzylamine with a direct two-electron transfer, resulting in the formation of benzene-methanimine. Benzenemethanimine then couples with unreacted benzylamine to get the final product of *N*-benzylidenebenzylamine. TEMPO⁺ then turns into TEMPOH and TEMPOH finally will be restored to TEMPO by O₂^{•−} produced by O₂ accepting conduction band electrons from TiO₂. It's worth noting that the HOMO level of adsorbate is a determining factor that causes a significant red-shift in the optical absorption region. TEMPO plays a key role in maintaining a normal operation of the whole photocatalytic system.

Furthermore, we recorded the electron transfer process of the **5-CH₃O-SA-TiO₂** complex by ESR spectra (Fig. 8). Before visible light irradiation, the conduction band electron signal is due to the surface oxygen vacancies of TiO₂ (Fig. 8, dark). However, 460 nm visible light irradiation led to the increase of conduction band electron signals due to LMCT (Fig. 8, 1.5 min). Further irradiation did not increase the signal (Fig. 8, 4.5 min). After switching off the visible light irradiation, the signal returned to its original state after transferring electron to O₂ (Fig. 8, O₂ 1 min).

Once the plausible mechanism for the cooperative photocatalysis system was established, we further investigated the breadth of visible

Table 6Visible light-driven selective oxidation of secondary amines into imines with air by merging **5-CH₃O-SA**-TiO₂ complex photocatalysis with TEMPO catalysis ^[a].

					
Entry	Substrate	Product	T(h)	Conv. [%]	Sel. [%]
1			2.0	87	69
2			1.5	78	67
3			1.5	77	74
4			2.0	78	68
5			3.0	79	56
6			3.0	72	58
7			3.0	61	53
8			3.0	30	93
9			3.0	12	72
10			3.0	52	83
11			3.0	37	85
12			3.0	27	86
13			3.0	30	73
14			2.0	62	70

[a] Reaction conditions: secondary amine (0.2 mmol), **5-CH₃O-SA** (0.0024 mmol), TiO₂ (50 mg), TEMPO (0.015 mmol), air (1 atm), blue LED irradiation (3 W × 4), CH₃CN (1 mL). [b] Determined by GC-FID using chlorobenzene as the internal standard, conversion of secondary amine, selectivity of corresponding imine.

light-driven selective oxidation of primary amines with air by merging **5-CH₃O-SA**-TiO₂ complex photocatalysis with TEMPO catalysis. The results are summarized in Table 5. Under the standard protocol of 0.8 mol% of **5-CH₃O-SA**, TiO₂ and 5 mol% of TEMPO, benzylamine and its derivatives are all oxidized into corresponding imines with air during 1 h or so reaction time (entries 1, 3–11, Table 5). More importantly, the gram-scale imine product can be obtained through our photocatalytic system merging **5-CH₃O-SA**-TiO₂ complex with TEMPO using atmosphere O₂ as an oxidant at room temperature. With 0.9 mmol benzylamine as the starting substrate, 92% yield of *N*-benzylidenebenzylamine (81 mg) is obtained in 3.5 h (entry 2, Table 5). The turnover number in terms of **5-CH₃O-SA** is 375. The **5-CH₃O-SA**-TiO₂ complex can be recycled twice with retaining 85% of activity (see Figure S6 for the XRD and DR-UV-vis spectra of the photocatalyst before and after use). Besides, the conversion of *p*-substituted benzylamines are superior to *m*-substituted benzylamines. Whether with electron-donating or electron-withdrawing substitutes, *p*-substituted benzyl amines can be efficiently transformed into imines with high conversions and selectivities (entries 3, 6, 7, 9–11, Table 5), which is in good agreement with the kinetic result of Hammett plot (Fig. 5b). In addition, heteroatomic methylamines can also be effectively transformed into imine as well (entries 12 and 13, Table 5). The attained results on selective oxidation of primary amines are very encouraging by the present system of cooperative photocatalysis.

Next we explored the scope of substrates to include secondary amines in further consideration of universality of the system comprised of **5-CH₃O-SA**-TiO₂ photocatalyst and TEMPO catalyst. The scope of the reactions is listed in Table 6 in which a broad range of secondary amines were favorably converted into their corresponding imines. We

noted that the oxidation of secondary benzyl amines has slower reaction rates and lower selectivities for imines compared with primary benzyl amines because of the steric hindrance effect. Nonetheless, the oxidation of many secondary benzyl amines can be obtained with moderate results. For example, the oxidation of these secondary benzyl amines with symmetrical structures or with relatively low steric hindrance can be achieved with higher conversions, although their selectivities for imines are lower than the case for the primary ones. They need longer time to react (entries 1–7, Table 6). For other secondary amines, their conversions are comparatively low. But higher selectivities for imines could be delivered based on the present photocatalytic system (entries 8–14, Table 6).

4. Conclusion

In summary, we have incorporated the use of **SA** and its derivatives as ligands for TiO₂ surface to enhance its visible light photocatalytic performance, and successfully applied it in the challenging reaction of selective oxidation of amines into imines with air. In this surface complex photocatalyst, the adsorbate can be viewed as a ligand to TiO₂ surface. Ligands always play an important role in transition-metal catalysts. Likewise, the ligand selection and design are also critical consideration to the activity of the surface complex photocatalysts. Amongst these tested **SA** and its derivatives, **5-CH₃O-SA** is the best ligand, attributing to the better cooperation between the photocatalytic cycle of **5-CH₃O-SA**-TiO₂ complex and the catalytic cycle of TEMPO. This advancement presents the details of interfacial interaction of surface complex on anatase TiO₂, which is very important for understanding and further development of visible light photocatalysis with

LMCT for selective chemical transformations.

Acknowledgments

This work was financially supported by the National Natural Science Foundation of China (grant numbers 21503086 and 21773173), the Fundamental Research Funds for the Central Universities (grant number 2042018kf0212) and the start-up fund of Wuhan University.

Appendix A. Supplementary data

Supplementary material related to this article can be found, in the online version, at doi:<https://doi.org/10.1016/j.apcatb.2018.11.090>.

References

- [1] H. Yamashita, K. Mori, Y. Kuwahara, T. Kamegawa, M.C. Wen, P. Verma, M. Che, *Chem. Soc. Rev.* 47 (2018) 8072–8096.
- [2] X.J. Lang, W.H. Ma, C.C. Chen, H.W. Ji, J.C. Zhao, *Acc. Chem. Res.* 47 (2014) 355–363.
- [3] H.J. Duchstein, H.J. Gurka, *Arch. Pharm.* 325 (1992) 129–146.
- [4] Y. Kim, B.G. Mun, A.L. Khan, M. Waqas, H.H. Kim, R. Shahzad, M. Imran, B.W. Yun, I.J. Lee, *PLoS One* 13 (2018) e0192650.
- [5] M. Kimura, T. Kawano, *Plant Signal. Behav.* 10 (2015) e1000145.
- [6] P.R. Guo, Z.H. Li, P.X. Huang, B.S. Li, S. Fang, J.F. Chu, H.W. Guo, *Plant Cell* 29 (2017) 2854–2870.
- [7] X.J. Lang, J.C. Zhao, X.D. Chen, *Angew. Chem. Int. Ed.* 55 (2016) 4697–4700.
- [8] X. Li, J.L. Shi, H.M. Hao, X.J. Lang, *Appl. Catal. B: Environ.* 232 (2018) 260–267.
- [9] H.M. Hao, Z. Wang, J.L. Shi, X. Li, X.J. Lang, *ChemCatChem* 10 (2018) 4545–4554.
- [10] Z. Wang, X.J. Lang, *Appl. Catal. B: Environ.* 224 (2018) 404–409.
- [11] X. Cao, Z. Chen, R. Lin, W.C. Cheong, S.J. Liu, J. Zhang, Q. Peng, C. Chen, T. Han, X.J. Tong, Y. Wang, R.G. Shen, W. Zhu, D.S. Wang, Y.D. Li, *Nat. Catal.* 1 (2018) 704–710.
- [12] D.G. Ma, A. Liu, S.H. Li, C.C. Lu, C.C. Chen, *Catal. Sci. Technol.* 8 (2018) 2030–2045.
- [13] G. Palmisano, E. García-López, G. Marci, V. Loddo, S. Yurdakal, V. Augugliaro, L. Palmisano, *Chem. Commun.* 46 (2010) 7074–7089.
- [14] C. Li, Y.F. Zhao, Y.Y. Gong, T. Wang, C.Q. Sun, *Phys. Chem. Chem. Phys.* 16 (2014) 21446–21451.
- [15] W.L. Wang, Z.F. Wang, J.J. Liu, Z. Luo, S.L. Sui, P. He, G.Q. Ding, Z.G. Zhang, L.Y. Sun, *Sci. Rep.* 7 (2017) 46610.
- [16] D. Tsukamoto, Y. Shiraishi, Y. Sugano, S. Ichikawa, S. Tanaka, T. Hirai, *J. Am. Chem. Soc.* 134 (2012) 6309–6315.
- [17] G. Zhang, G. Kim, W. Choi, *Energy Environ. Sci.* 7 (2014) 954–966.
- [18] M.M. Medić, M. Vasić, A.R. Zarubica, L.V. Trandafilović, G. Dražić, M.D. Dramićanin, J.M. Nedeljković, *RSC Adv.* 6 (2016) 94780–94786.
- [19] W. Macyk, K. Szaciłowski, G. Stochel, M. Buchalska, J. Kunciewicz, P. Łabuz, *Coord. Chem. Rev.* 254 (2010) 2687–2701.
- [20] M.S. Ata, Y. Liu, I. Zhitomirsky, *RSC Adv.* 4 (2014) 22716–22732.
- [21] K.L. Orchard, D. Hojo, K.P. Sokol, M.J. Chan, N. Asao, T. Adschiri, E. Reisner, *Chem. Commun.* 53 (2017) 12638–12641.
- [22] T. Kamegawa, H. Seto, S. Matsuura, H. Yamashita, *ACS Appl. Mater. Interfaces* 4 (2012) 6635–6639.
- [23] P. Karthik, R. Vinoth, S.G. Babu, M.C. Wen, T. Kamegawa, H. Yamashita, B. Neppolian, *RSC Adv.* 5 (2015) 39752–39759.
- [24] J.L. Shi, H.M. Hao, X. Li, X.J. Lang, *Catal. Sci. Technol.* 8 (2018) 3910–3917.
- [25] L. Li, Y.J. Feng, Y.Z. Liu, B. Wei, J.X. Guo, W.Z. Jiao, Z.H. Zhang, Q.L. Zhang, *Appl. Surf. Sci.* 363 (2016) 627–635.
- [26] S.X. Li, F.Y. Zheng, W.L. Cai, A.Q. Han, Y.K. Xie, *J. Hazard. Mater.* 135 (2006) 431–436.
- [27] X. Wang, H.M. Zhao, X. Quan, Y.Z. Zhao, S. Chen, *J. Hazard. Mater.* 166 (2009) 547–552.
- [28] M. Sboui, M.F. Nsib, A. Rayes, T. Ochiai, A. Houas, C.R. Chim., 20 (2017) 181–189.
- [29] J.M. de Souza e Silva, M. Pastorello, M. Strauss, C.M. Maroneze, F.A. Sigoli, Y. Gushikem, I.O. Mazali, *RSC Adv.* 2 (2012).
- [30] R.R. Ma, X.J. Wang, J.Y. Huang, J.K. Song, J. Zhang, X. Wang, *Vacuum* 141 (2017) 157–165.
- [31] J.H. Kou, C.H. Lu, J. Wang, Y.K. Chen, Z.Z. Xu, R.S. Varma, *Chem. Rev.* 117 (2017) 1445–1514.
- [32] X.J. Lang, J.C. Zhao, X.D. Chen, *Chem. Soc. Rev.* 45 (2016) 3026–3038.
- [33] X.J. Lang, J.C. Zhao, *Chem. Asian J.* 13 (2018) 599–613.
- [34] A.E. Regazzoni, P. Mandelbaum, M. Matsuyoshi, S. Schiller, S.A. Bilmes, M.A. Blesa, *Langmuir* 14 (1998) 868–874.
- [35] S. Varaganti, G. Ramakrishna, *J. Phys. Chem. C* 114 (2010) 13917–13925.
- [36] X.J. Lang, W.H. Ma, Y.B. Zhao, C.C. Chen, H.W. Ji, J.C. Zhao, *Chem. Eur. J.* 18 (2012) 2624–2631.
- [37] I.A. Janković, Z.V. Šaponjić, M.I. Čomor, J.M. Nedeljković, *J. Phys. Chem. C* 113 (2009) 12645–12652.
- [38] C.I. Oprea, P. Panait, M.A. Gîrțu, *Beilstein J. Nanotechnol.* 5 (2014) 1016–1030.
- [39] D.T. Sawyer, J.S. Valentine, *Acc. Chem. Res.* 14 (1981) 393–400.
- [40] C.M. Li, G. Chen, J.X. Sun, Y.J. Feng, J.J. Liu, H.J. Dong, *Appl. Catal. B: Environ.* 163 (2015) 415–423.
- [41] C.M. Li, G. Chen, J.X. Sun, J.C. Rao, Z.H. Han, Y.D. Hu, W.N. Xing, C.M. Zhang, *Appl. Catal. B: Environ.* 188 (2016) 39–47.
- [42] C.M. Li, Y. Xu, W.G. Tu, G. Chen, R. Xu, *Green Chem.* 19 (2017) 882–899.
- [43] C.M. Li, S.Y. Yu, H.J. Dong, C.B. Liu, H.J. Wu, H.N. Che, G. Chen, *Appl. Catal. B: Environ.* 238 (2018) 284–293.
- [44] C.M. Li, S.Y. Yu, H.J. Dong, Y. Wang, H.J. Wu, X.X. Zhang, G. Chen, C.B. Liu, *J. Colloid Interface Sci.* 531 (2018) 331–342.
- [45] C.M. Li, S.Y. Yu, Y. Wang, J. Han, H.J. Dong, G. Chen, *J. Taiwan Inst. Chem. Eng.* 87 (2018) 272–280.